AMSE Association for the Advancement of Modelling & Simulation Techniques in Enterprises
IIETA International Information and Engineering Technology Association
Advancing the World of Information and Engineering

Advances in Modelling and Analysis C
Vol. 73, No. 3, September, 2018, pp. 112-122
Journal homepage: http://iieta.org/Journals/AMA/AMA_C

Analysis of Math function based controller combined with PID for solar-powered electric vehicle

Raghavaiah Katuri[1*], Srinivasarao Gorantla[2]

[1] Department of Electrical and Electronics Engineering, Vignan's Foundation for Science, Technology, and Research, Vadlamudi, Guntur 522213, Andhra Pradesh, India
[2] Electrical and Electronics Engineering, Vignan's Foundation for Science, Technology, and Research, Vadlamudi, Guntur 522213, Andhra Pradesh, India

Corresponding Author Email: rk_eeep@vignanuniversity.org

http//doi.org/10.18280/ama_c.730306

Received: 19 July 2018
Accepted: 25 August 2018

Keywords:
solar power, Hybrid Electric Vehicles (HEVs), Electric Vehicles (EVs), Bidirectional Converter (BDC), Unidirectional Converter (UDC), battery, ultracapacitor, Math Function Based (MFB) controller, Proportional Integral Derivative (PID) controller

ABSTRACT

Hybrid Energy Storage System (HESS) powered electric vehicles (EVs)/ hybrid electric vehicles (HEVs) have its own advantages than single power source fed EVs/HEVs. The battery and ultracapacitor (UC) combination forms the HESS, battery always acts as the main source whereas UC full fill the auxiliary power sources requirement by supporting the battery during transient and starting period of the electric vehicle. In any HESS powered electric vehicle, smooth transition between the energy sources is the major obstacle according to the vehicle dynamics. The main aim of this work is to design a new control strategy for a smooth transition between the energy sources in HESS. Four math functions are taken and programmed individually based on the speed of an electric motor termed as Math Function Based (MFB) controller, thereafter the designed MFB controller is combined with conventional Proportional Integral Derivative (PID) controller to achieve the main objective of this work, and the combination MFB plus PID called as a hybrid controller. The MFB controller always regulates the pulse signal generated by the PID controller to the Bidirectional converter (BDC) as well as a Unidirectional converter (UDC) according to the speed of the electric motor. In this work additionally, the solar panel is added to the electric vehicle to charge the battery during the sunlight availability timings depending upon the irradiance and temperature. The entire solar-powered electric vehicle circuit is modeled and analyzed in four modes with different loads according to the speed of an electric motor. All modes of results are discussed, presented in simulation results and discussion section.

1. INTRODUCTION

Nowadays electric vehicles are extensively used in the world for the transport system to save the atmosphere from the harmful gases. But the problem associated with the electric vehicle is charging stations are not that much established and are taking more time to charge the energy source. PV panels are used to charge the battery in electric vehicle continuously whenever it required [1]. A solar power station is proposed for electric vehicle charging, generally many electric vehicles are fed with self-charge mechanism containing with its own PV panel. The designed solar power station can be useful if a vehicle own power is not sufficient to charge the battery [2-3]. Both EVs and HEVs are having various technical problems associated with their main energy source that may be battery or fuel cell. Generally, small size batteries are inefficient to meet the transient power requirement of the electric vehicle especially during climbing of hill areas and cold start of the motor because of battery low specific power inherent property [5]. On another hand, UCs are having high specific power as an advantage along with the low specific energy, which indicates that battery and UC are having opposite characteristics. At present all available energy sources are having the high energy density to drive the electric vehicle, and don't have high power density. The high energy density of a source enhances the driving range and high power density can provide the quick power to the vehicle during transient periods. In order to obtain the efficient energy source for electric vehicle hybridization of both the source are required [9-14].

The hybrid controller is designed by combining MFB with a different conventional controller. By using the designed controller switching between battery and UC is done based on the speed of an electric motor [5-6]. Different characteristics multiple sources are combined with the hybridization concept for electric vehicle application. Here UC and battery are combined and forms HESS with average power can pump by the battery on other hand peak power can be feed by UC. HESS improves the life cycle of battery by dismissing the number of charging and discharging periods, this can be achieved with UC only. The efficient combination UC and battery forms better energy storage system than the conventional single battery or fuel cell by fulfilling the all road condition of the electric vehicles [6-10].

To fulfill the unexpected driver behavior and different load condition, HESS is designed with various artificial intelligence techniques. Researchers mostly concentrating on the optimal usage of fuels which used to drive the electric vehicles mainly on batteries and different algorithms are proposed to find the optimal way of utilizing the energy sources [13-14].

For small urban electric vehicles, energy management architecture is developed and different characteristics contained energy sources are integrated like high power

density and high energy density. For proper energy splitting between two energy sources rule-based metaheuristic controller is designed by considering different load conditions on the electric vehicle [4].

A new HESS is developed with low rating DC-DC converter further it can be compared with conventional HESS, which is having large power rating DC-DC converter topology. In the designed HESS battery end maintains lower voltage value where UC end maintains higher voltage value. Here UC will supplies the power to the drive until its voltage level is less than the battery voltage level, with that comparative constant load is created for the battery [16]. In addition, the battery is not used to directly harvest energy from the regenerative braking; thus, the battery is isolated from frequent charges, which will increase the life of the battery

A modified soft switching method is suggested for BDC as well as UDC with coupled inductors. Hysteresis current controller is used for zero voltage switching up to the maximum load range [17]. An effective energy storage system is developed for HEVs/EVs with the neural network controller and the suggested system reduces the energy requirement of the electric vehicle [18].

An effective control strategy is designed to provide the crest power requirement from UC within 20sec. In remaining all cases average power can be supplied by a battery for electric vehicle [19]. A polynomial is used for better power management between UC and battery. Here battery is connected directly to the dc link whereas UC is connected through BDC to dc link. PIC18F4431 microcontroller is used for a DC-DC converter for proper power-sharing [20]. A new control strategy is designed and implemented, to switch the energy sources present in the HESS according to the electric vehicle dynamics [21].

The main aim of this work is to design a hybrid controller by combining the MFB controller with PID controller to obtain a smooth switching between the battery and UC. Additionally PV panel is connected to the model to charge the battery during sunlight available timings. This work is structured as follows. Section II Presents PV array mathematical modeling. Section III Presents the proposed system model. Section IV describes the Math function based controller. Modes of operation of converter model presented in section V. Section VI presents the proposed model control strategy. Section VII describes simulation results and discussions. Finally, the main conclusions are presented in section VIII.

2. PROPOSED SYSTEM MODEL

Figure 1 represents the block diagram model of the HESS including a solar panel for battery charging during sunlight available time. Here the MFB controller and conventional PID controller outputs are compared at the circuit breaker section and send the required pulse signal to the converters according to the electric motor speed. The PID controller always generates the pulse signal to BDC as well as UDC by comparing reference and the actual voltage level of the converters. On another hand, MFB controller regulates the pulse signals generated by the PID based on the speed of an electric motor. The UC supply the transient power requirement of the motor whereas battery can supply the average power to the motor.

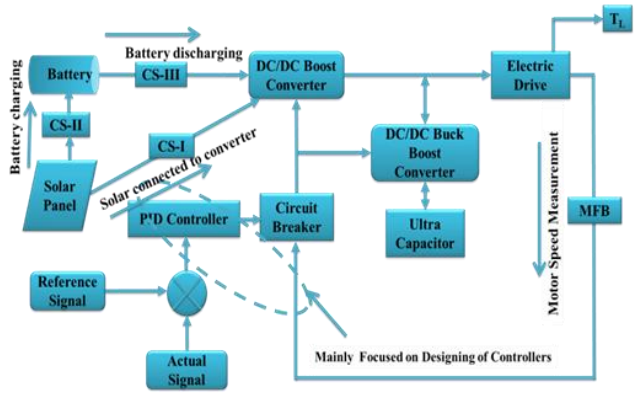

Figure 1. Proposed block diagram model of the hybrid energy Storage system

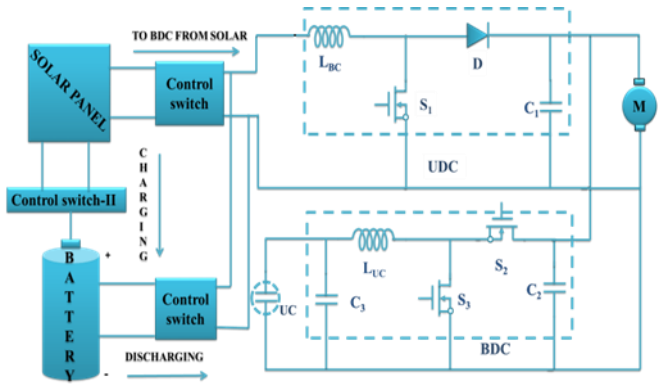

Figure 2. Converter model circuit diagram with HESS

Above figure 2 represents that the converter model circuit diagram of HESS which consisting of the Bidirectional converter (BDC), Unidirectional converter (UDC), battery, Ultracapacitor (UC) and solar panel with three switches named as S_1, S_2, S_3. The switch S_1 is always in ON condition except for a heavy load condition. Here the solar panel is connected to UDC as well as a battery through control switches I, II. The batteries are connected to UDC through control switch-III. Here the battery charging and discharging states are controlled by the control switches ON and OFF conditions. The major part of power can be supplied by the battery, on another hand auxiliary power can be supplied by UC that may be starting and transit period of the electric motor.

3. PV ARRAY MATHEMATICAL MODELING

One PV cell is capable of generates an output voltage of less than 1 V i.e. each Si Photovoltaic cell develops the output voltage of around 0.7 V during open circuit time and 0.5 V under working condition. No. of cells are connected in series and parallel to form a PV module and a number of modules are allied in series and parallel to produce the required output. Using Si-based photovoltaic modules the PV system converts only 15% of solar energy into electricity. Ideal solar PV cell is demonstrated by a current source and an inverted diode coupled in parallel to it as shown in Figure 3.

The current source represents the current generated by photons denoted as I_{cell} and its output is constant under constant temperature and constant light incident radiation. The practical behavior of the cell is deviated from ideal due to the

optical and electrical losses. There are two key parameters as short-circuit current (I_{sc}) and open circuit voltage that is frequently used to characterize a PV cell. By short-circuiting the terminals of the cell the photon generated current as shown in Figure 3(b), flows out of the cell called as a short circuit current (I_{sc}). Thus, we can say that $I_{cell} = I_{sc}$ as the current I_{cell} is flowing in a single series circuit. As the terminals are short-circuited then the voltage across the circuit is equal to zero i.e. $V_{oc} = 0$ and the short-circuit current is the PV cell load current (or the output current which is very maximum as equal to that of the current source or photovoltaic photon generated current i.e. $I_{cell} = I_{sc} = I_m$ Similarly, when the terminals are open circuited i.e. no load and nothing is connected as represented in 3 (c), the load current of a PV cell becomes zero. And the load voltage of a PV cell is equal to the maximum applied source voltage or open circuit voltage i.e. ($V_m = V_{oc}$).

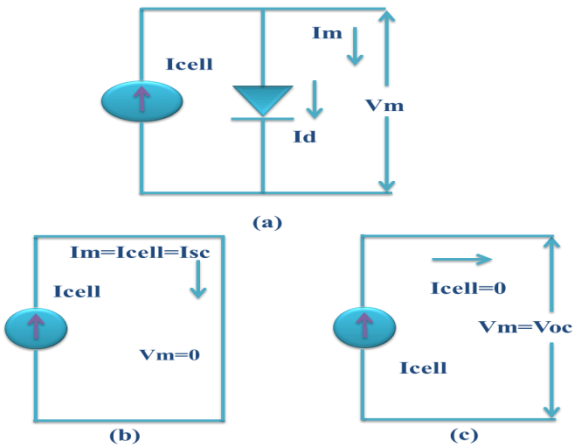

Figure 3. (a) PV cell equivalent circuit, (b) PV cell at short circuit condition (c) PV cell at open circuit condition

The PV cell output current can found by applying KVL to circuit 1(a),

$$I_m = I_{cell} - I_d \quad (1)$$

The current through diode can be represented with bellow equation

$$I_d = I_{rscell}\left[e^{\left(\frac{QV}{KTap}\right)-1}\right] \quad (2)$$

By replacing Id in Equation 2, it gives the current-voltage relationship of the PV cell as shown below

$$I_m = I_{cell} - I_{rscell}\left[e^{\left(\frac{QV}{KTap}\right)-1}\right] \quad (3)$$

The diode reverse saturation current (I_{rscell}) is constant under the constant temperature and irradiance that is calculated by the open circuit condition of PV cell as illustrated in Figure 3(b). From the Equation (3) it is observed that $I_m = 0$ and solve for I_{rscell}

$$I_{rscell} = \frac{I_{cell}}{\left[e^{\left(\frac{QV}{KTap}\right)-1}\right]} \quad (4)$$

The photon generated current is directly proportional to the irradiance and temperature, whereas the voltage is directly proportional to the irradiance and inversely proportional to the temperature. The value of I_{scr} is provided by the manufacturer datasheet at STC (standard test condition). At STC, the working temperature and irradiance are 25^0 C and 1000 W/m respectively.

In the present work, the standard PV array is taken and generated the power with different temperature, irradiance values. Thereafter using DC-DC converter solar panel voltage changed according to the electric vehicle requirement. Here tree control switches are connected to the solar panel, battery, and UDC. State of charge of the battery and the output voltage of the solar panel decides the control switches action. Finally, the power required by the electric vehicle can be fulfilled using solar power based on the availability of sunlight.

4. MATH FUNCTION BASED CONTROLLER (MFB)

The designed hybrid controller is a combination of MFB controller and PID controller. The PID controller generates the pulse signals whereas the MFB controller regulates the pulse signals according to the speed of the electric motor. The MFB controller generates the controls signal in four modes as follows.

(i) If the speed of the motor is less than or equal to 4800 rpm then MFB generates signal U_1 as 1.
(ii) If the speed is in between 4600 to 4800 rpm then MFB generates signals U_1 and U_2 as 1.
(iii) If the speed of the motor lies between 4801rpm to 4930 rpm MFB generates signal U_3 as 1.
(iv) If the speed of the motor is greater than or equal to 4931 rpm MFB generates signal U_4 as 1.

All the above signals are used to perform the smooth switching between the battery and UC which means switching between sources can be done by means of MFB controller combined with the PID controller. Here U_1, U_2, U_3, and U_4 are the output signals generated by the MFB controller based on the speed of an electric motor.

5. MODES OF OPERATION OF CONVERTER MODEL

The proposed work is analyzed in four modes with different loads. All four modes with different loads and switches ON and OFF condition illustrated in below table 1.

Table 1. Load condition based switching action

Mode	S_1	S_2	S_3	Load Torque
I	OFF	OFF	ON	Heavy Load
II	ON	OFF	ON	Medium Load
III	ON	OFF	OFF	Rated load
IV	ON	ON	OFF	No Load

4.1 Mode-I operation

During mode-I operation a heavy load is applied to the electric motor and entire power is supplied by the UC only. And the switch S_3 only in ON condition, remain switches S_1, S_2 are in OFF position. Here the battery gets charged from the solar panel depending on control switches operation. In this mode of operation total power will flows from UC to the load.

In this work, the battery gets charged from the solar panel during sunlight available timings and discharges the same amount of energy to the electric motor during no irradiance and temperature period.

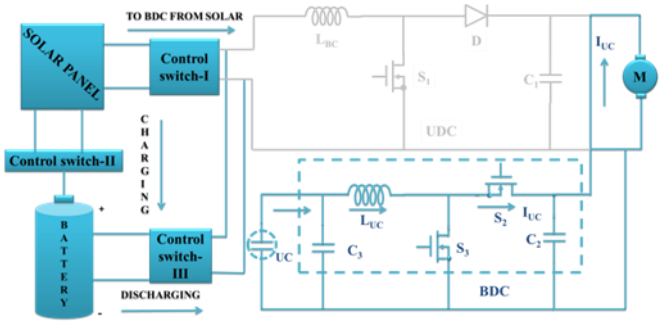

Figure 4. Converter Mode-I circuit diagram with HESS

4.2 Mode-II operation

Mode-II related to the slightly more than rated load condition on the electric motor. The battery and UC together supply the required power to the electric motor, which means UC will reduce the extra burden on the battery. So switches S_1 and S_3 are in ON position, remain switch S_2 is in OFF position. In this work, the battery gets charged from the solar panel during sunlight available timings and discharges the same amount of energy to the electric motor during no irradiance and temperature period. Finally, in this mode of operation, the power will flow from battery, UC to an electric motor.

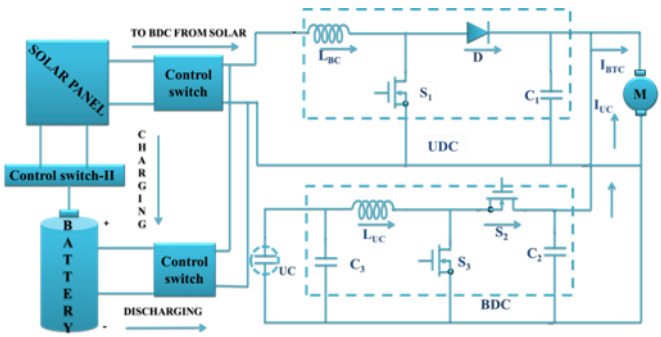

Figure 5. Converter Mode-II circuit diagram with HESS

4.3 Mode-III operation

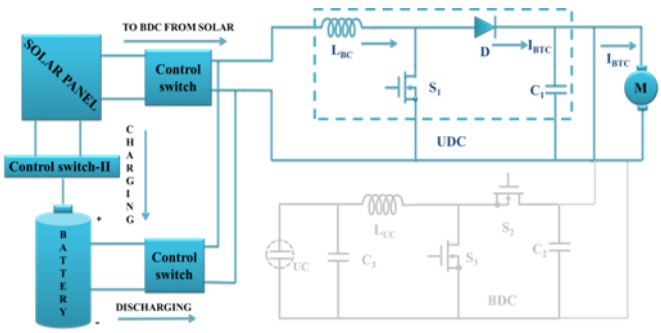

Figure 6. Converter Mode-III circuit diagram with HESS

This mode is related to the rated load on the electric motor, so switch S_1 is in ON position and remain switches S_2, S_3 are in OFF position. During rated load condition motor requires average power only, which can be supplied by the battery itself. In this work, the battery gets charged from the solar panel during sunlight available timings and discharges the same amount of energy to the electric motor during no irradiance and temperature period. Finally, in this mode of operation, the power flows from the battery to the electric motor.

4.4 Mode-IV operation

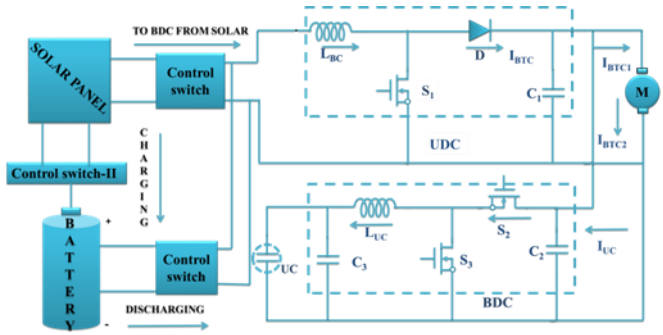

Figure 7. Converter Mode-IV circuit diagram with HESS

A light load or no load is applied to the electric motor during mode-IV operation. In this mode, the motor requires less amount of power that may be less than average power supply the battery. So total no-load power is supplied by the battery itself, additionally, battery also supplies energy to the UC for charging. Switches S_1, S_2 are in ON condition and remain switch S_3 is in OFF condition. In this work, the battery gets charged from the solar panel during sunlight available timings and discharges the same amount of energy to the electric motor during no irradiance and temperature period. In this mode of operation, the power flows from battery to the electric motor as UC for charging.

6. PROPOSED MODEL CONTROL STRATEGY

The proposed control strategy is designed with a hybrid controller which can generate the pulse signal to BDC as well as UDC according to the speed of an electric motor. During mode-I operation pulse signals are generated to only BDC working as a boost converter and no pulse signals are generated to the UDC. In mode-II operation pulse signals are generated to BDC as well as UDC, both are working in boost mode. During mode-III operation the pulse signals are generated to UDC only and no pulse signal to BDC. Finally, in mode-IV operation pulse signals are generated to BDC works under buck mode for UC charging and UDC as a boost converter. All above mention operation happen only with a hybrid controller action.

(1) During starting of a motor and heavy loaded condition UC supplies require power to the load. In this mode, the math function U_1 gives signal value as 1 and remaining all math functions generates a signal as 0 because during this period the speed of the motor is $\leq$ 4800 rpm. The converter operates based on all math function generated signals. The converters in operation are the boost converter at the UC end.

(2) When the power demanded by the load is beyond the designed range of the battery output power, UC will assist the battery to deliver power to the motor. In this mode of

operation, motor speed is from 4600 rpm to 4800 rpm. Hence MFB generates U_1 and U_2 pulse signals as 1 and generates U_3 and U_4 pulse signals as 0. The converters in operation are the boost converter at the battery end and the boost converter at the UC end.

(3) When battery output power matches the desired power of the motor, the battery individually supplies the power to the motor. In this mode of operation, the speed of the motor is from 4801 rpm to 4930 rpm. Hence MFB generates a U_3 pulse signal as 1 and generates U_1, U_2 and U_4 pulse signals as 0. During this time, the UDC at the battery terminal works.

(4) When battery provides more power than the motor need, the extra power will be used to charge the UC. So the power of the battery will flow into both the UC and the motor. In this mode of operation, motor speed is >4931 rpm. Hence MFB generates a U_4 pulse signal as 1 and generates U_1, U_2 and U_3 pulse signals as 0. According to the converters designed, the UDC at the battery end and the buck converter (BDC) at the UC end will work in this scenario.

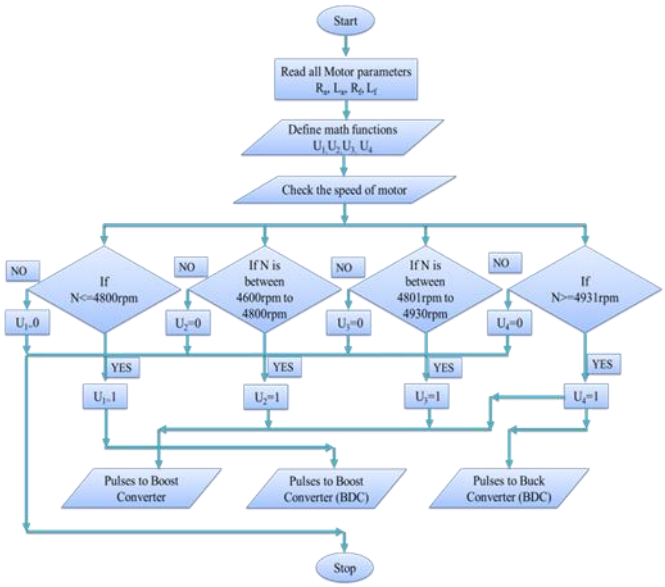

Figure 8. Flowchart of the control strategy

The converters pulse signals are generated to individual switches by the MFB plus PID controller combination, based on the speed of the electric motor explained with the help of bellow figure's 9, 10 and 11.

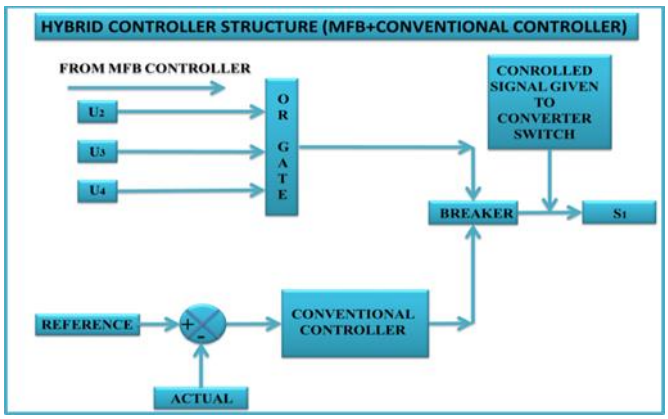

Figure 9. Pulse signals generated structure to switch ONE present in UDC

Figure 9 is the structure related to a pulse signal generated to switch S_1 based on the speed of the electric motor. Here S_1 is related to the UDC, which is connected at the battery end. The pulse signals U_2, U_3 and U_4 generated by the MFB controller are given to the OR gate, which means if the speed of the electric motor is more than 4600 rpm then MFB controller signals are in the active state further this signal can be compared with the signal generated by the conventional controller. Here the conventional PID controller can generate the pulse signal by comparing the reference as well as actual voltage signals of UDC. Finally, the controlled signal of S_1 is generated after the successful comparison between the MFB signals as well as the PID controller signal by means of the breaker. In this way, the pulse signal of switch S_1 can be controlled based on the speed of the electric motor speed by the Hybrid controller (combination of MFB plus PID). Here the main aim of designed MFB controller is to achieve control action of switches based on the speed of the electric motor for a smooth transition between battery and UC. The designed hybrid controller always works based on the speed of an electric motor for precise switching action between energy sources; this can be taken advantage for proper power splitting between the battery and UC during normal as well transient periods of an electric vehicle.

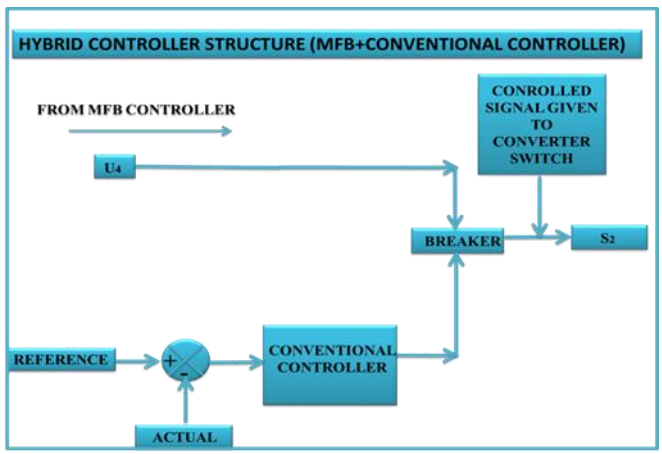

Figure. 10. Pulse signals generated structure to switch TWO present in BDC

Figure 10 is the structure related to a pulse signal generated to switch S_2 based on the speed of the electric motor. Here S_2 is related to the BDC, which is connected at the UC end. The pulse U_4 is generated by the MFB controller is given to breaker block directly which means if the speed of the electric motor is more than 4931 rpm then MFB control signal is in the active state, further this signal compared with the pulse signal generated by the conventional PID controller. Here the conventional PID controller generates the pulse signal based on the actual as well as reference voltage signals of BDC. Finally, the controlled signal of switch S_2 is generated after comparison between the MFB signal as well as PID controller signal. Here the aim of designed MFB controller is to achieve control action of switches based on the speed of the electric motor for a smooth transition between battery and UC. The designed hybrid controller always works based on the speed of an electric motor for precise switching action between energy sources; this can be taken advantage for proper power splitting between the battery and UC during normal as well transient periods of an electric vehicle.

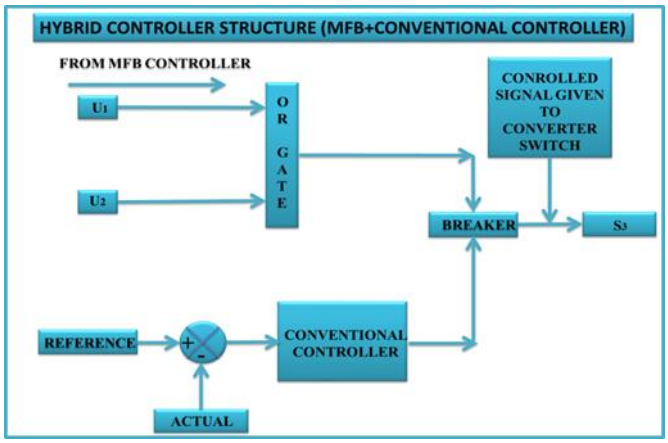

Figure 11. Pulse signals generated structure to switch THREE present in BDC

Figure 11 is the structure related to a pulse signal generated to switch S_3 based on the speed of the electric motor. Here the switch S_3 is related to the BDC, which is connected at the UC end. The pulse signals U_1 and U_2 are generated by the MFB controller and given to the OR gate, which means if the speed of an electric motor is between 4600 rpm 4800 rpm then MFB control signal will be in the active state, further those signals are compared with the signal generated by the conventional controller. Here the conventional PID controller generates the pulse signals based on the actual as well as reference voltage signals of the BDC. Finally, the comparison has been made between the MFB signal and PID controller signal, after that the controlled signal of switch S_3 can be generated. The main aim of the designed MFB controller is to achieve control action of switches based on the speed of the electric motor for a smooth transition between battery and UC. The designed hybrid controller always works based on the speed of an electric motor for precise switching action between energy sources; this can be taken advantage for proper power splitting between the battery and UC during normal as well transient periods of an electric vehicle.

7. SIMULATION RESULTS AND DISCUSSIONS

7.1 Mode-I results

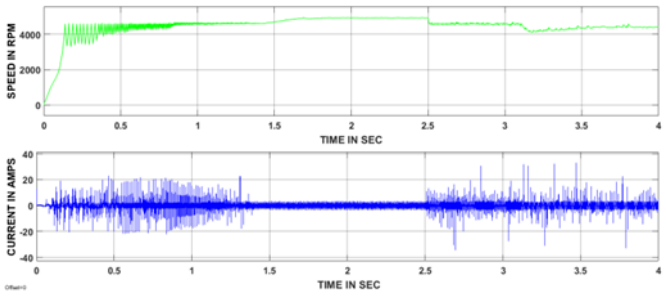

Figure 12. The speed and current responses of the electric motor during a heavy load condition

The speed and current responses of the electric motor during a heavy load condition are represented with the figure 12. During starting, motor speed response is reached the steady state at 1.6 sec. Thereafter there are no distortions in the current as well as the speed responses. At 2.5 sec a heavy load is applied to the electric motor, due to that the motor speed reduced to less than 4600 rpm and current value increased more than the rated value. Due to heavy load, the speed response has not reached the steady state within the specified time period.

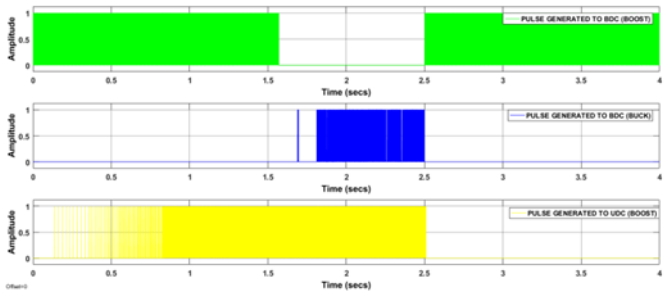

Figure 13. The pulse signals generated by the MFB with PID controller during a heavy load condition

Generally, peak power can be supplied by UC during a heavy load condition on the electric motor. During starting of motor pulse signals are generated to only BDC working as a boost converter after some time motor attains speed more than 4600 rpm, from that point again pulse signals are generated to UDC working as a boost converter. Again after some time, motor speed reaches more than 4930 rpm, during this time pulse signal are generated to both BDC as a buck and UDC as a boost converter. At 2.5 sec a heavy is applied to the motor due to that the speed of the motor decreased to less than 4600 rpm and current also raised more than the rated value. During this condition, peak power can be supplied by the UC by generating pulse signals to only BDC working as a boost converter.

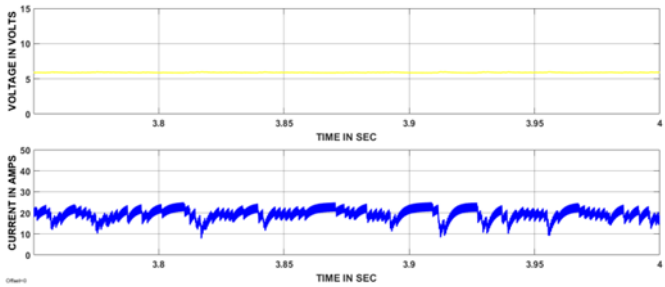

Figure 14. UDC input voltage and current responses during a heavy load condition

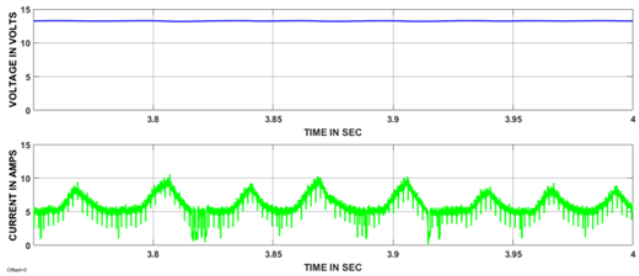

Figure 15. UDC output voltage and current responses during a heavy load condition

The input voltage and current responses of UDC during a heavy load condition are shown in figure 14. Here input of UDC is obtained from the battery parameters because the output of the battery is connected as an input of UDC. The input voltage is maintained 6V and current also changes

according to the load changes on the electric motor.

The output voltage of UDC is boosted to 12V according to the electric motor requirement, corresponding to the boosted voltage output current also changes. The output of the UDC is connected to the load side.

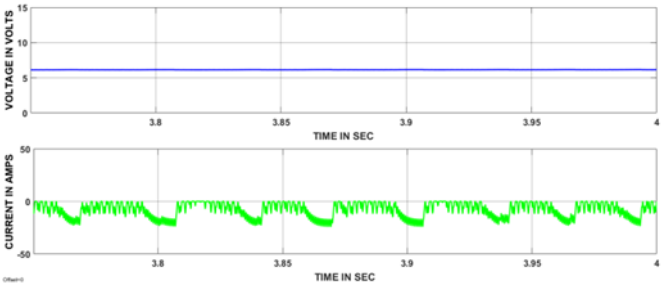

Figure 16. BDC input voltage and current responses during a heavy load condition

Here the input side of UC is considered as a BDC input whereas load side is considered as a BDC output. So the input side of BDC resembles the UC parameter values only. The input voltage of BDC is maintained 6V and the current value varies according to the load changes.

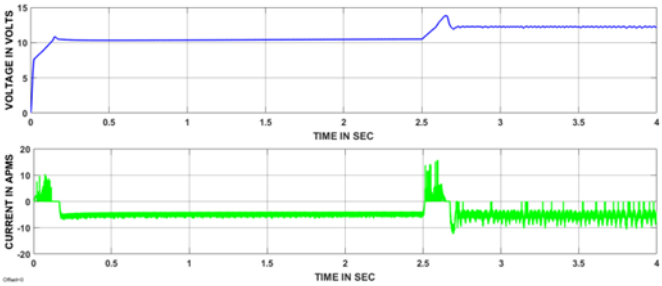

Figure 17. BDC output voltage and current responses during a heavy load condition

Above figure 17 represents that the BDC output voltage and current responses. During starting and the sudden load applied conditions, the motor draws more current than its rated value. In such cases to provide the transient power to motor UC assists the battery to improve the life of the battery. And remaining all cases UC gets charged. UC current shows negative value during charging period on another hand positive current indicating that discharging period.

7.2 Mode-II results

The speed and current responses of the electric motor during a slightly more than rated load condition are represented with the figure 18. The motor speed response is reached the steady state at 1.6 sec. Thereafter there are no changes present in the current as well as the speed responses. At 2.5 sec slightly more than the rated load is applied to the electric motor, due to that the motor speed maintained between 4600 rpm to 4800 rpm and current value increased slightly more than the rated value. Due to slightly more than rated load, the speed response reached the steady state within 0.6 sec by the designed controller action.

During starting of motor pulse signals are generated to only BDC, working under boost mode, after some time motor attains speed more than 4600 rpm, from that point on words pulse signals are generated to UDC working as a boost converter. Again motor speed reaches more than 4930 rpm, during that period pulse signal are generated to both BDC as a buck and UDC as a boost converter. At 2.5 sec slightly more than rated load is applied to the motor due to that the speed of the motor maintained between 4600 rpm to 4800 rpm and current value increased to slightly more than the rated value. The peak power can be supplied by the UC by generating pulse signals to only BDC working as a boost converter and average power can be supplied by the battery by generating pulses to UDC as a boost converter.

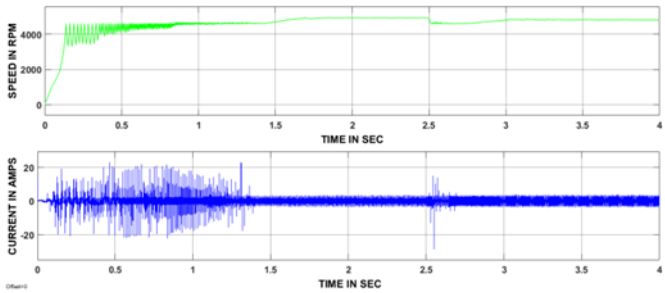

Figure 18. The speed and current responses of the electric motor during slightly more than rated load condition

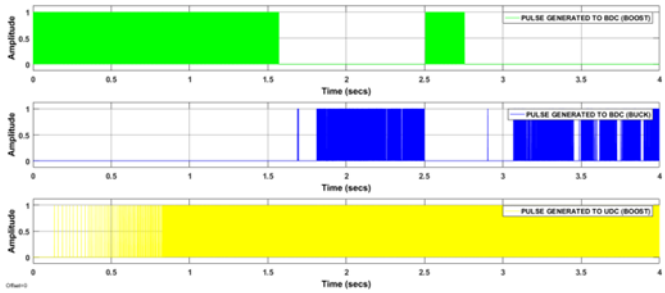

Figure 19. The pulse signals generated by the MFB with PID controller during slightly more than rated load condition

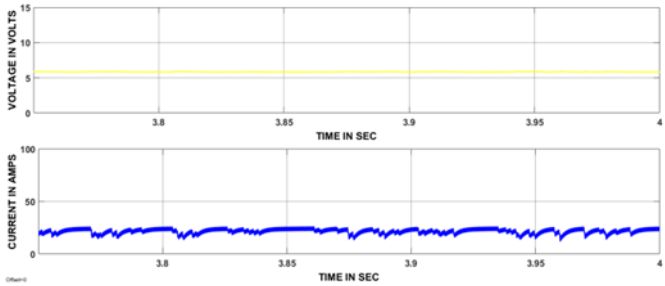

Figure 20. UDC input voltage and current responses during slightly more than rated load condition

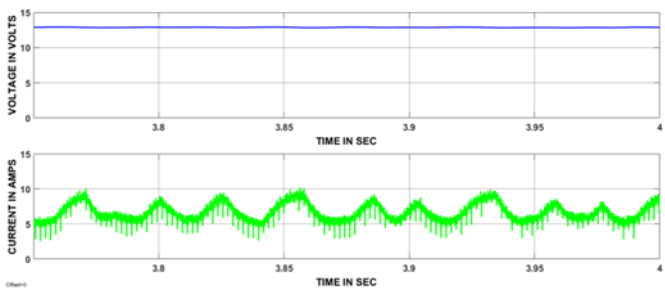

Figure 21. UDC output voltage and current responses during slightly more than rated load condition

The input voltage and current responses of UDC during slightly more than rated load condition are shown in figure 20. Here input of UDC is obtained from the battery parameters because the output of the battery is connected as an input of UDC. The input voltage is maintained 6V and current also changes according to the load changes on the electric motor.

The output voltage of UDC is boosted to 12V according to the electric motor requirement, corresponding to the boosted voltage output current also changes. The output of the UDC is connected to the load side.

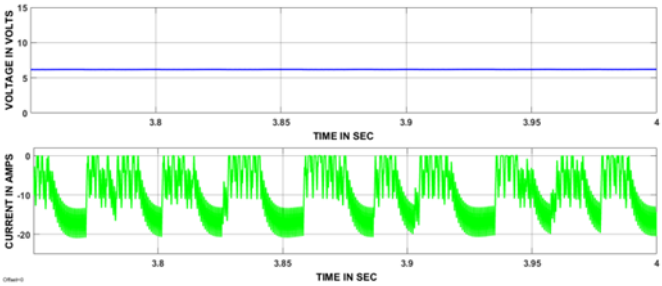

Figure 22. BDC input voltage and current responses during slightly more than rated load condition

Here the input side of UC is considered as a BDC input whereas load side is considered as a BDC output. So the input side of BDC resembles the UC parameter values only. The input voltage of BDC is maintained 6V and the current value varies according to the load changes.

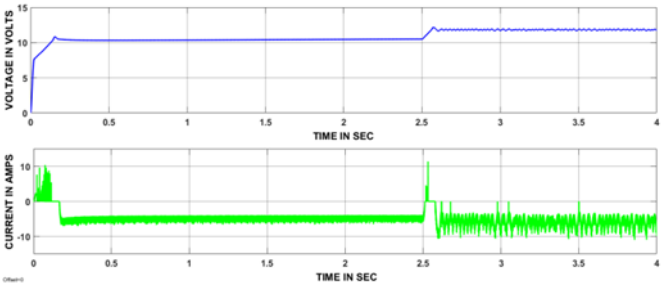

Figure 23. BDC output voltage and current responses during slightly more than rated load condition

Above figure 23 represents that the BDC output voltage and current responses. During starting and the sudden load applied conditions, the motor draws more current than its rated value. In such cases to provide the transient power to motor UC assists the battery to improve the life of the battery. And remaining all cases UC gets charged. UC current shows negative value during charging period on another hand positive current indicating that discharging period.

7.3 Mode-III results

The speed and current responses of an electric motor during a rated load condition can be represented with the figure 24. The motor speed response has reached the steady state at 1.6 sec. Thereafter there are no distortions present in the current as well as the speed responses. At 2.5 sec rated load is applied to the electric motor, due to that the motor speed maintained between 4801 rpm to 4930 rpm and current value raised to the rated value. Due to the rated load, the speed response will reach the steady state within 0. 4sec by the designed controller action.

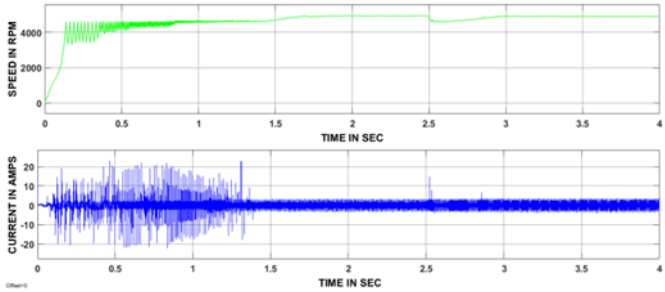

Figure 24. The speed and current responses of the electric motor during a rated load condition

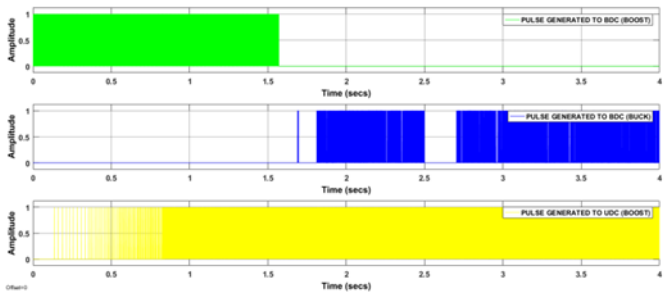

Figure 25. The pulse signals generated by the MFB with PID controller during a rated load condition

During starting of motor pulse signals are generated to BDC working as a boost converter after some time motor attains speed more than 4600 rpm, from that point on words pulse signals are generated to UDC working as a boost converter. Thereafter motor speed reaches to more than 4930 rpm, during that time pulse signals are generated to both BDC as a buck and UDC as a boost converter. At 2.5 sec a rated load is applied to the motor, due to that the speed of an electric motor maintained between 4801 to 4930 rpm and current also increased to the rated value. During this period average power can be supplied by the battery itself by generating a pulse signal to UDC as a boost converter and no pulse signal generated to BDC.

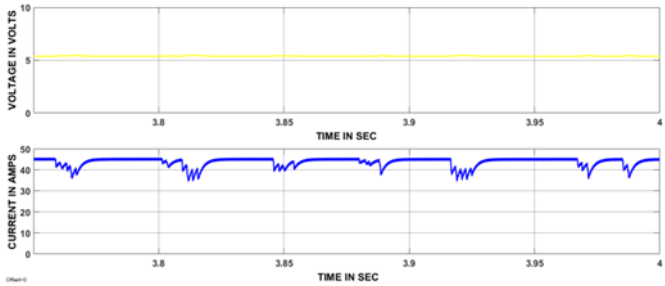

Figure 26. UDC input voltage and current responses during a rated load condition

The input voltage and current responses of UDC during rated load condition are shown in figure 26. Here input of UDC is obtained from the battery parameters because the output of the battery is connected as an input of UDC. The input voltage is maintained 6V and current also changes according to the load changes on the electric motor.

The output voltage of UDC is boosted to 12V according to the electric motor requirement, corresponding to the boosted voltage output current also changes. The output of the UDC is connected to the load side.

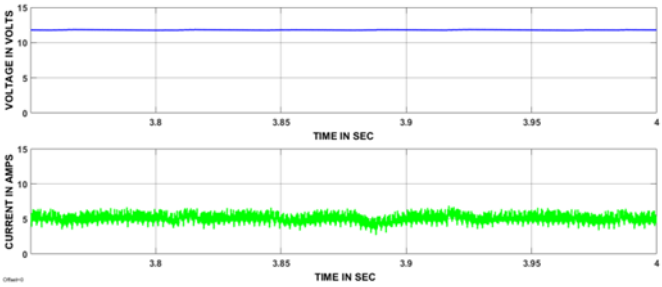

Figure 27. UDC output voltage and current responses during a rated load condition

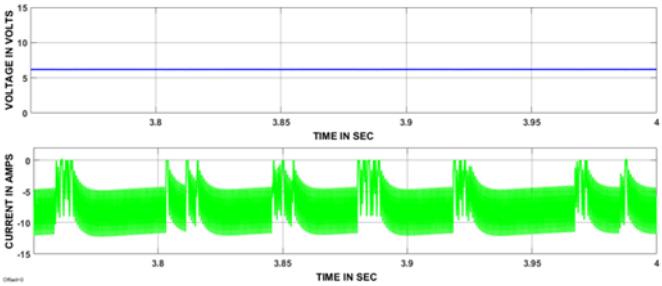

Figure 28. BDC input voltage and current responses during a rated load condition

Here the input side of UC is considered as a BDC input whereas load side is considered as a BDC output. So the input side of BDC resembles the UC parameter values only. The input voltage of BDC is maintained 6V and the current value varies according to the load changes.

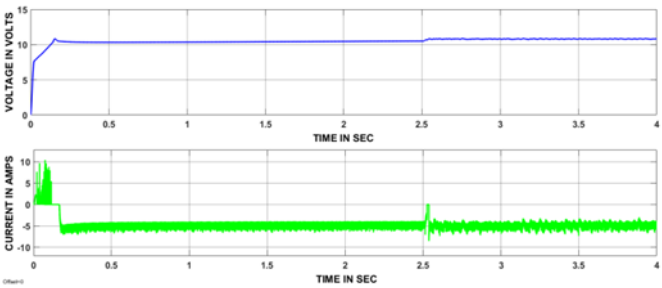

Figure 29. BDC output voltage and current responses during a rated load condition

Above figure 29 represents that the BDC output voltage and current responses. During starting and the sudden load applied conditions, the motor draws more current than its rated value. In such cases to provide the transient power to motor UC assists the battery to improve the life of the battery. And remaining all cases UC gets charged. UC current shows negative value during charging period on another hand positive current indicating that discharging period.

7.4 Mode-IV results

The speed and current responses of an electric motor during a rated load condition can be represented with the figure 30. The motor speed response has reached the steady state at 1.6 sec. Thereafter there are no distortions present in the current as well as the speed responses. In this mode of operation, no load is applied to the motor, so there are no changes in speed and current responses until any type of load applied to the motor.

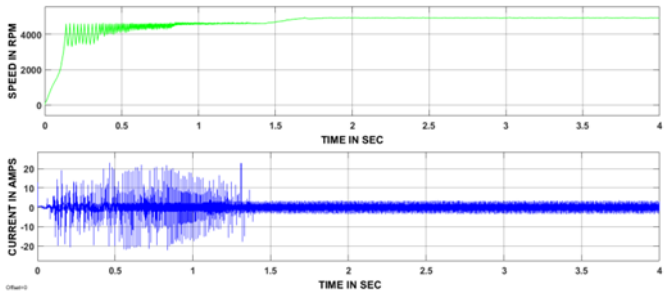

Figure 30. The speed and current responses of the electric motor during no load condition

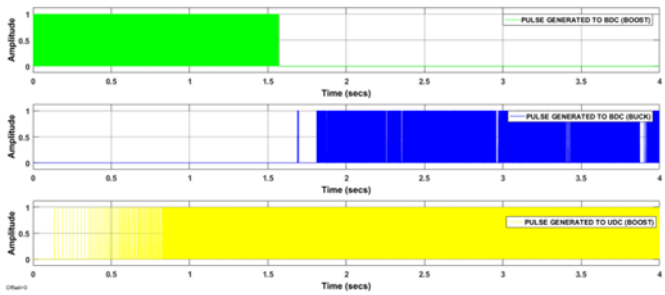

Figure 31. The pulse signals generated by the MFB with PID controller during no load condition

During starting of motor pulse signals are generated to only BDC working as a boost converter after some time motor attains speed more than 4600 rpm, from that point again pulse signals are generated to UDC working as a boost converter. Thereafter the motor speed reaches more than 4930 rpm, from this period on words pulse signals are generated to both BDC as a buck and UDC as a boost converter. In this mode of operation, no load is applied to the electric motor so pulse signals are continuously generated to BDC as a buck converter for UC charging and UDC as a boost converter until load applied to the motor.

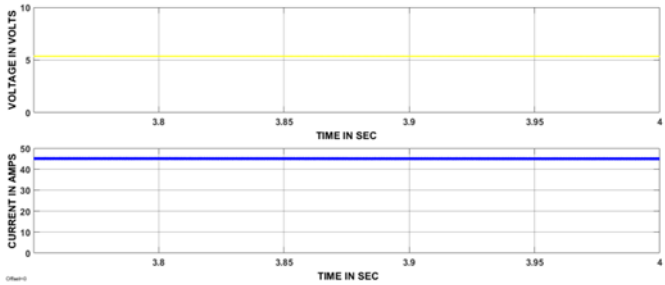

Figure 32. UDC input voltage and current responses during no load condition

The input voltage and current responses of UDC during no load condition are shown in figure 32. Here input of UDC is obtained from the battery parameters because the output of the battery is connected as an input of UDC. The input voltage is maintained 6V and current also changes according to the load changes on the electric motor.

The output voltage of UDC is boosted to 12V according to the electric motor requirement, corresponding to the boosted voltage output current also changes. The output of the UDC is connected to the load side.

The input side of UC is considered as a BDC input whereas load side is considered as a BDC output. So the input side of

BDC resembles the UC parameter values only. The input voltage of BDC is maintained 6V and the current value varies according to the load changes.

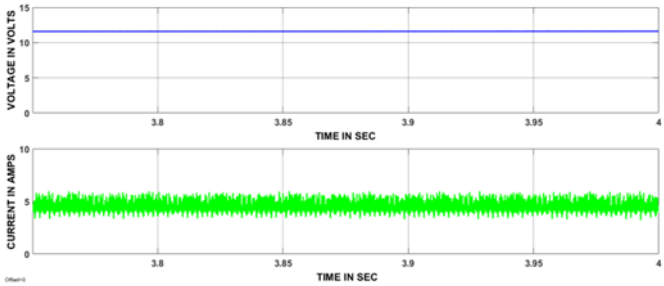

Figure 33. UDC output voltage and current responses during no load condition

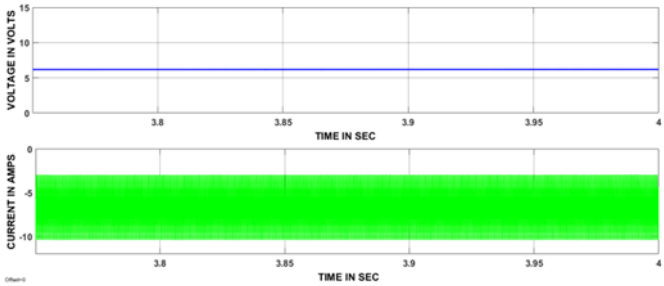

Figure 34. BDC input voltage and current responses during no load condition

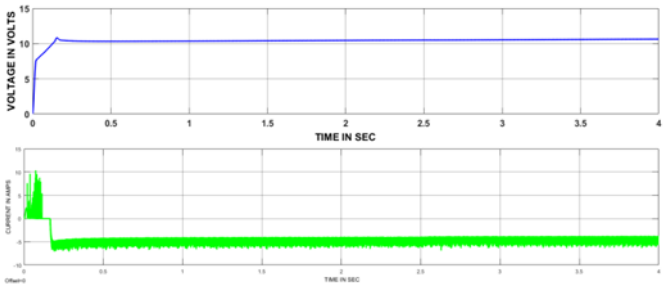

Figure 35. BDC output voltage and current responses during no load condition

Above figure 35 represents that the BDC output voltage and current responses. During starting motor draws more current than its rated value. In such cases to provide the transient power to motor UC assists the battery to improve the life of the battery. And remaining all cases UC gets charged. UC current shows negative value during charging period on another hand positive current indicating that discharging period.

7.5 Battery parameters

In this paper battery minimum SOC is taken as 20%, if battery SOC is below 20% then it should get charged from the solar power directly. Thereafter battery discharges the same amount of energy to the electric vehicle until its SOC reaches to 20%. From the above figure 36, it is clear that during discharging time the battery current showing positive whereas showing negative value under the charging period.

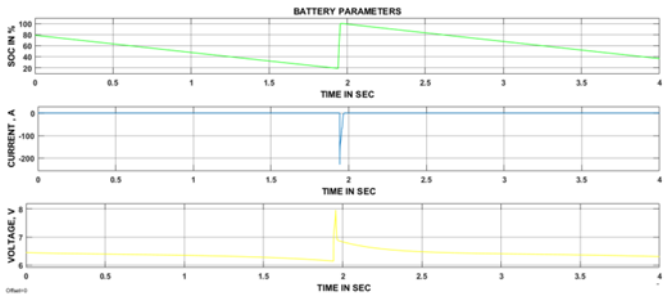

Figure 36. The battery parameters during charging and discharging periods

7.6 Solar panel parameters

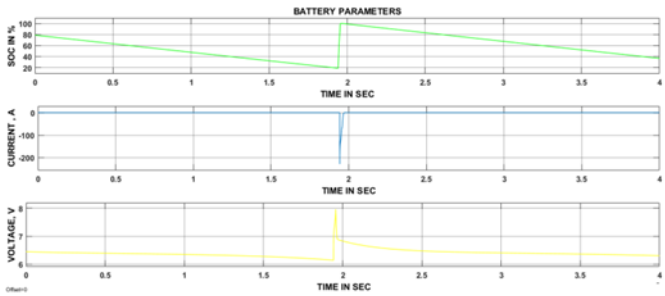

Figure 37. Solar panel parameters and duty cycle of the converter

Figure 37 represents the solar panel input parameters and duty cycle value. Solar energy is generated based on the availability of sunlight and irradiance. Here the different quantity of power is generated with different voltage levels by changing the irradiance and temperature. The duty cycle of the converter also changes according to changes in temperature and irradiance which is connected at solar panel end, in order to maintain maximum power at converter secondary end. Different variations of temperature and irradiance can be observed from the above figure 37.

Table 2. Operation of the converter based on four modes

Mode Condition	UDC	BDC	Mode of Operation
Mode-1	Off	Boost	Power flow UC to Motor
Mode-2	Boost	Boost	Power flow UC+Battery to Motor
Mode-3	Boost	Off	Power flow Battery to Motor
Mode-4	Boost	Buck	Power Flow to Motor and UC From Battery

Table 3. State of math function based on the speed of the motor

Condition Based on Speed of the Motor	State of Math Function
If Speed is ≤4800 rpm	Math function U_1=1
If Speed is from 4600 rpm To 4800 rpm	Math function U_1=1& U_2=1
If Speed is from 4801 rpm To 4930 rpm	Math function U_3=1
If Speed is >4931 rpm	Math function U_4=1

8. CONCLUSIONS

The hybrid controller is designed for HESS powered solar electric vehicle for a smooth transition between battery and UC. The designed controller is a combination of MFB with conventional PID controller, and both the controllers worked together and given satisfactory results during load changing from heavy load to light load. The conventional PID controller generated the pulse signals required by BDC as well as UDC, whereas MFB controller regulated those signals according to the speed of an electric motor with the help of four math functions U_1, U_2, U_3, and U_4. The battery gets charged from solar power during sunlight availability and discharged the same amount of energy during the absence of irradiance and temperature based on the action of connected control switches between solar panel to battery. The battery charging and discharging plots also presented along with four modes of operation of the electric motor with different loads, in simulation and discussion section.

REFERENCES

[1] Khan S, Ahmad A, Ahmad F, Shafaati Shemami M, Saad Alam, M., & Khateeb, S. (2018). A comprehensive review on solar-powered electric vehicle charging system. Smart Science 6(1): 54-79.

[2] Sadagopan, S, Banerji S, Vedula P, Shabin M, Bharatiraja C. (2014, April). A solar power system for electric vehicles with maximum power point tracking for novel energy sharing. In India Educators' Conference (TIIEC), 2014 Texas Instruments. IEEE, pp. 124-130

[3] Bhavnani SH. (1994). Design and construction of a solar-electric vehicle. Journal of Solar Energy Engineering 116(1): 28-34.

[4] Golchoubian P, Azad NL. (2017). Real-time nonlinear model predictive control of a battery–supercapacitor hybrid energy storage system in electric vehicles. IEEE Transactions on Vehicular Technology 66(11): 9678-88. http://dx.doi.org/10.1109/TVT.2017.2725307

[5] Katuri R, Gorantla SR. (2018). Math function based controller applied to the electric/hybrid electric vehicle. Modeling, Measurement and Control A 91(1): 15-21.

[6] Katuri R, Rao G. (2018). Design of math function based controller for smooth switching of hybrid energy storage system. Majlesi Journal of Electrical Engineering 12(2): 47-54.

[7] Shen J, Khaligh A. (2015). A supervisory energy management control strategy in a battery/ultracapacitor hybrid energy storage system. IEEE Transactions on Transportation Electrification 1(3): 223-31. http://dx.doi.org/10.1109/TTE.2015.2464690

[8] Wu D, Todd R, Forsyth AJ. (2015). Adaptive rate-limit control for energy storage systems. IEEE Transactions on Industrial Electronics 62(7): 4231-40. http://dx.doi.org/10.1109/TIE.2014.2385043

[9] Emadi A, Lee YJ, Rajashekara K. (2008). Power electronics and motor drives in electric, hybrid electric, and plug-in hybrid electric vehicles. IEEE Transactions on industrial electronics 55(6): 2237-2245. http://dx.doi.org/10.1109/TIE.2008.922768

[10] Chan CC, Bouscayrol A, Chen K. (2010). Electric, hybrid, and fuel-cell vehicles: Architectures and modelling. IEEE transactions on vehicular technology 59(2): 589-598. http://dx.doi.org/10.1109/TVT.2009.2033605

[11] Xiang C, Wang Y, Hu S, Wang W. (2014). A new topology and control strategy for a hybrid battery-ultra-capacitor energy storage system. Energies 7(5): 2874-96. http://dx.doi.org/3390/en7052874

[12] Gholizadeh M, Salmasi FR. (2014). Estimation of state of charge, unknown nonlinearities, and state of health of a lithium-ion battery based on a comprehensive unobservable model. IEEE Transactions on Industrial Electronics 61(3): 1335-1344. http://dx.doi.org/10.1109/TIE.2013.2259779

[13] Sánchez Ramos L, Blanco Viejo CJ, Álvarez Antón JC, García García VG, González Vega M, Viera Pérez JC. (2015). A variable effective capacity model for LiFePO4 traction batteries using computational intelligence techniques. IEEE Transactions on Industrial Electronics 62(1). http://dx.doi.org/10.1109/TIE.2014.2327552

[14] de Castro R, Araujo RE, Trovao JPF, Pereirinha PG, Melo P, Freitas D. (2012). Robust DC-link control in EVs with multiple energy storage systems. IEEE Transactions on Vehicular Technology 61(8): 3553-3565. http://dx.doi.org/10.1109/TVT.2012.2208772

[15] Carter R, Cruden A, Hall PJ. (2012). Optimizing for efficiency or battery life in a battery/supercapacitor electric vehicle. IEEE Transactions on Vehicular Technology 61(4): 1526-33. http://dx.doi.org/10.1109/TVT.2012.2188551

[16] Ferreira AA, Pomilio JA, Spiazzi G, de Araujo Silva L. (2008). Energy management fuzzy logic supervisory for electric vehicle power supplies system. IEEE Transactions on Power Electronics 23(1): 107-115. http://dx.doi.org/10.1109/TPEL.2007.911799

[17] Choi ME, Kim SW, Seo SW. (2012). Energy management optimization in a battery/supercapacitor hybrid energy storage system. IEEE Transactions on Smart Grid. 3(1): 463-72. http://dx.doi.org/10.1109/TSG.2011.2164816

[18] Trovao JPF, Santos VD, Antunes CH, Pereirinha PG, Jorge HM. (2015). A real-time energy management architecture for multisource electric vehicles. IEEE Trans. Industrial Electronics 62(5): 3223-3233. http://dx.doi.org/10.1109/TIE.2014.2376883

[19] Cao J, Emadi A. (2012). A new battery/ultracapacitor hybrid energy storage system for electric, hybrid, and plug-in hybrid electric vehicles. IEEE Transactions on Power Electronics 27(1): 122-132. http://dx.doi.org/10.1109/TPEL.2011.2151206

[20] Zhang Y, Sen PC. (2003). A new soft-switching technique for buck, boost, and buck-boost converters. IEEE Transactions on Industry Applications 39(6): 1775-1782. http://dx.doi.org/10.1109/TIA.2003.818964

[21] Katuri R, Gorantla S. (2018). Simulation and modelling of math function based controller implemented with fuzzy and artificial neural network for a smooth transition between battery and ultracapacitor. Advances in Modelling and Analysis C 73(2): 45-52.